Annals of Nuclear Medicine Vol. 16, No. 6, 431–435, 2002

Attenuation correction of myocardial SPECT images with X-ray CT: Effects of registration errors between X-ray CT and SPECT

Yasuyuki TAKAHASHI,* Kenya MURASE,* Hiroshi HIGASHINO,**
Teruhito MOCHIZUKI*** and Nobutoku MOTOMURA****

*Department of Medical Engineering, Division of Allied Health Sciences, Osaka Graduate School of Medicine
**Department of Radiology, Ehime Prefectural Imabari Hospital
***Department of Radiology, Ehime University School of Medicine
****Toshiba Medical Engineering Laboratory

Purpose: Attenuation correction with an X-ray CT image is a new method to correct attenuation on SPECT imaging, but the effect of the registration errors between CT and SPECT images is unclear. In this study, we investigated the effects of the registration errors on myocardial SPECT, analyzing data from a phantom and a human volunteer. ***Methods:*** Registerion (fusion) of the X-ray CT and SPECT images was done with standard packaged software in three dimensional fashion, by using linked transaxial, coronal and sagittal images. In the phantom study, an X-ray CT image was shifted 1 to 3 pixels on the *x*, *y* and *z* axes, and rotated 6 degrees clockwise. Attenuation correction maps generated from each misaligned X-ray CT image were used to reconstruct misaligned SPECT images of the phantom filled with ^{201}Tl. In a human volunteer, X-ray CT was acquired in different conditions (during inspiration vs. expiration). CT values were transferred to an attenuation constant by using straight lines; an attenuation constant of 0/cm in the air (CT value = –1,000 HU) and that of 0.150/cm in water (CT value = 0 HU). For comparison, attenuation correction with transmission CT (TCT) data and an external γ-ray source (^{99m}Tc) was also applied to reconstruct SPECT images. ***Results:*** Simulated breast attenuation with a breast attachment, and inferior wall attenuation were properly corrected by means of the attenuation correction map generated from X-ray CT. As pixel shift increased, deviation of the SPECT images increased in misaligned images in the phantom study. In the human study, SPECT images were affected by the scan conditions of the X-ray CT. ***Conclusion:*** Attenuation correction of myocardial SPECT with an X-ray CT image is a simple and potentially beneficial method for clinical use, but accurate registration of the X-ray CT to SPECT image is essential for satisfactory attenuation correction.

Key words: SPECT, X-ray CT, fusion image, misaligned images

INTRODUCTION

A PATIENT SPECIFIC ATTENUATION CORRECTION MAP is necessary for better attenuation correction in myocardial single photon emission tomography (SPECT), since the thorax is a non-uniform structure, having several kinds of organs with different attenuation values. For this purpose, transmission CT (TCT) with an external γ-ray source was proposed to obtain the patient's specific attenuation correction map,[1] but TCT requires an expensive external radiation source such as ^{153}Gd or ^{241}Am, and hardware and software.[2] Although ^{99m}Tc could be used as an external γ-ray source, Japanese regulations do not allow us to divert ^{99m}Tc as an external γ-ray source. Attenuation correction with TCT is reported to increase specificity in the inferior wall (right coronary artery territory), but it has a tendency to over correct the attenuation that has caused

Received September 17, 2001, revision accepted July 10, 2002.

For reprint contact: Yasuyuki Takahashi, Department of Radiology, Ehime Prefectural Imabari Hospital, 4–5–5, Ishii-cho, Imabari, Ehime 794–0006, JAPAN.

E-mail: i-y-taka@epnh.pref.ehime.jp

a count decrease in the antero-apical wall in some cases, i.e., possibility to cause a false positive in the left anterior ascending artery territory. Therefore, its clinical usefulness is still controversial and application is limited to the practice of myocardial SPECT.

Recently, with hybrid X-ray CT and SPECT, an attenuation correction method was proposed from an attenuation constant map produced by simultaneous acquisition of X-ray CT and SPECT images,[3,4] but the number of institutions that can use the expensive system is limited. The idea to use X-ray CT to produce an attenuation map for attenuation correction was applied to the separate X-ray CT and SPECT systems.[5] In such a case, accurate image registration (fusion) of X-ray CT and SPECT images would be essential for reliable attenuation correction.

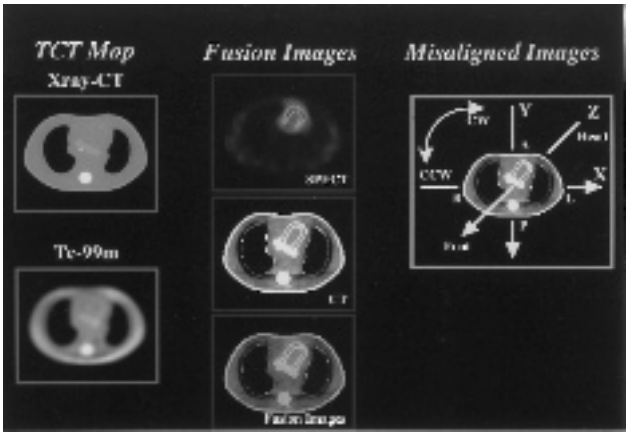

Fig. 1 Overview of the systems used and illustration for registration errors (shift). *Left:* TCT map by X-ray CT and ^{99m}Tc using an external γ-ray source. *Center:* Registration (fusion) of the images by the three-dimensional method. *Right:* Direction of pixel shifting.

In the present study, attenuation correction of ^{201}Tl myocardial SPECT images was conducted with X-ray CT images. We investigated the effect of the registration errors of the images by two methods in a phantom study. We also investigated the influence of different X-ray CT scan conditions.

As a control, the TCT attenuation correction method was performed with ^{99m}Tc as an external γ-ray source.

MATERIALS AND METHODS

SPECT system

The SPECT system used was a GCA-9300A/UI (Toshiba Medical Systems, Tochigi, Japan) equipped with one cardiac fan beam collimator and two parallel beam collimators, with which TCT data were acquired by using an external gamma-ray source and ^{201}Tl myocardial SPECT data for the phantom and a human subject were acquired (Fig. 1, lower left). The TCT external radiation source was a sheet-shape made from a bellows tube filled with 740 MBq of ^{99m}Tc. The tube was 1 mm in inner diameter and made of fluorocarbon resin embedded in an acrylic rectangular board measuring 30 cm × 10 cm. Both TCT and SPECT images were sampled with a matrix size of 128 × 128, step and shoot mode (30 sec/direction) at intervals of 6 degrees (60 directions, 360-degree collection in total). Pixel size was 3.2 mm. SPECT images were reconstructed by ordered subset-expectation maximization (OSEM: Iteration No. 10, Subsets 5)[6] after 15 × 15-point smoothing. The projections were reconstructed with a ramp convolution filter, and high frequency noise was decreased with post-reconstruction Butterworth filtering (cutoff = 0.44 cycle/cm, power factor = 8).

X-ray CT system

The X-ray CT system used was a ProSeed-SA (GE-

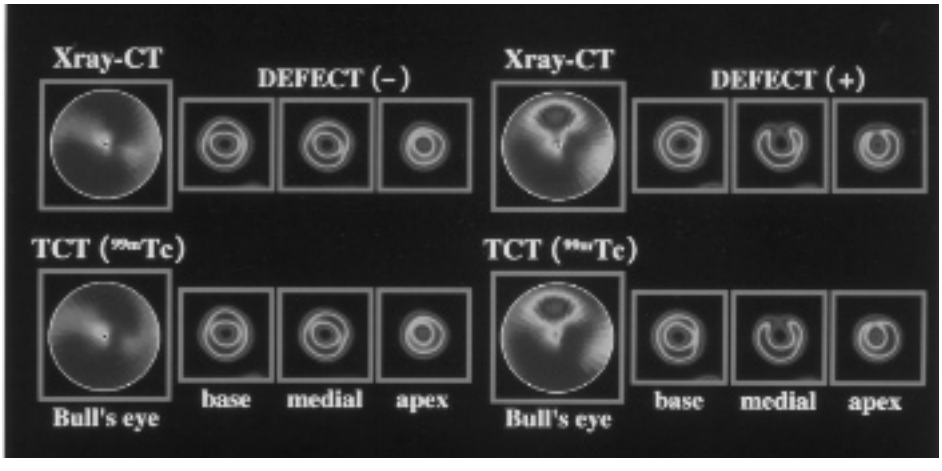

Fig. 2 Attenuation corrected Bull's eye map and short axis images in the phantom study. *Left:* without defects. *Right:* with defects.

Yokogawa Medical Systems, Tokyo, Japan) at a tube voltage of 140 kV and a tube electric current of 200 mA. In the phantom study, slice thickness was 5 mm and rotation speed was 0.8 sec/rotation. In the human study, X-ray CT was scanned with three different condition protocols. (1) Holding his breath on inspiration, slice thickness of 10 mm, and 3.0 sec/rotation with table feed of 10 mm/rotation. (2) Holding his breath on expiration, slice thickness of 10 mm, and 3.0 sec/rotation with table feed of 10 mm/rotation.

Transformation of CT values to attenuation coefficient

In both phantom and human studies, X-ray CT data were acquired with a 512×512 matrix, then the images were resized to a 128×128 matrix to match the SPECT images. CT values (HU) were transferred into an attenuation constant with straight lines; an attenuation constant of 0/cm in the air (CT value = −1,000 HU) and those of 0.150/cm (^{99m}Tc) or 0.187/cm (^{201}Tl) in water (CT value = 0 HU). The image conversion was carried out by straight line approximation ($\mu = 1.5 \times$ CT value $\times 10^{-4} + 0.15$)[7] (Fig. 1, upper left).

Myocardial phantom

The myocardial phantom (Data Spectrum Corp., Hillsborough, NC) was tested with and without a defect (20×20 mm) in the anterior wall. The uniformity of the myocardium was evaluated with the images without the defect. The concentration of ^{201}Tl in the myocardial part was 92.5 kBq/m*l*. Reproducibility (extent and severity) of the defect was also compared.

Registration of X-ray CT image to SPECT image

As registration of the image, three point sources of ^{201}Tl 5 mm in diameter were adhered to the axillae and navel on the myocardial phantom (Data Spectrum Corp., Hillsborough, NC). X-ray CT and SPECT images were fused and registered with packaged software (Automatic Registration Tool: ART)[8] (Fig. 1, center). The software can automatically scale the images from the actual length of the pixels and the position of the table, producing sagittal images; then determining several corresponding points and minimizing deviations on the coordination of these points by successive approximation, but the landmarks (3 point sources) were put on the body for manual operation, when the registration error in the images was visible.

To examine the magnitude of the registration errors on generating the attenuation map, or the images reconstructed with the misregistered attenuation map, X-ray CT (Fig. 1, right) images were shifted 1 to 3 pixels on the *x*, *y* and *z* axes or 2 to 6° counterclockwise. Then the transverse images generated with the misregistered attenuation maps were compared with images generated with a non-shifted attenuation map.

For comparison, the normalized root mean square error

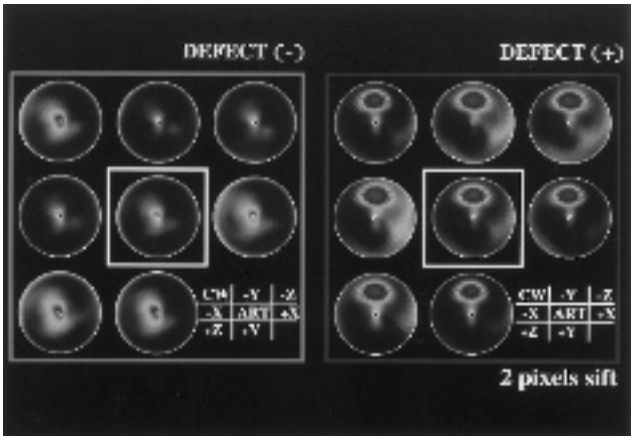

Fig. 3 Bull's eye maps with and without registration errors (shift: 6 pixels in *x*, *y* and *z* axes, and 4° in clockwise direction). ART: Automatic Registration Tool.

Table 1 Bull's eye map without registration error created by the three-dimensional registration. The NRMSE (%) was calculated using image with registration errors (shifts)

NRMSE (%)	Translation (3 mm/pixel)			Rotation (2°/pixel)	
	x-axis	*y*-axis	*z*-axis	CW	CCW
+3 pixels	6.89	4.97	9.39	—	3.35
+2 pixels	4.65	3.34	5.71	—	2.53
+1 pixel	1.50	1.73	1.82	—	1.50
ART	—	—	—	—	—
–1 pixel	2.53	1.60	1.60	1.53	—
–2 pixels	3.75	3.48	2.77	3.20	—
–3 pixels	5.00	4.31	3.71	3.50	—

[NRMSE (%): $\Sigma(X_i - O_i)^2/\Sigma O_i^2$, X_i: Measurement image, O_i: Standard image, i: pixel number ($i = 1 \sim n$)] by the Bull's eye map was used in the image evaluation of the phantom study.

To quantify the uniformity, we divided the Bull's eye map into 48 sectors. The mean of the normalized SPECT value and the SD of the 48 sectors were calculated.

RESULTS

Figure 2 shows the results on the attenuation corrected Bull's eye map and short axis images in the phantom study. NRMSE of the TCT to X-ray CT was 2.53 (Fig. 2, left). As the shift increased on the standard image of ART, deviations of the NRMSE increased (Fig. 3, left. Table 1). The extent of the defect area increased in proportion to the shift and rotation (Fig. 3, right).

In the human study, the attenuation corrected Bull's eye map with inspiration X-ray CT was corrected with the Bull's eye map by means of TCT better than with expiration X-ray CT (Fig. 4). Mean normalized SPECT values were as follows: TCT (87.5 ± 6.4, mean ± SD), inspiration

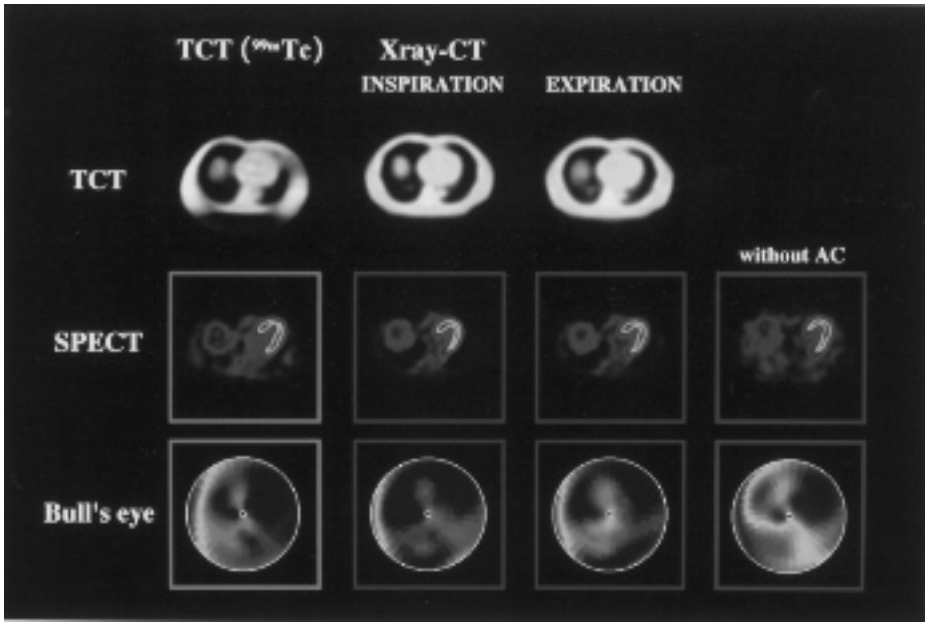

Fig. 4 Difference of the scanning protocol of the X-ray CT of a healthy subject, TCT map, SPECT image, and Bull's eye map are shown.

X-ray CT (87.0 ± 5.8), expiration X-ray CT (86.0 ± 7.4), and without attenuation correction (82.7 ± 9.9). The SD of the SPECT value normalized with inspiration X-ray CT was the smallest (best uniformity).

DISCUSSION

In this study, we corrected the attenuation of myocardial SPECT images with an attenuation correction map generated from X-ray CT images. By means of the DICOM (Digital Imaging and Communications in Medicine) standard, we could use X-ray CT and SPECT by different manufacturers. There was no difficulty in using the SPECT registration software.

Attenuation of myocardial SPECT in the inferior wall and antero-septal wall was properly corrected, and uniform myocardial SPECT images were obtained. The homogeneity and the count ratio of the defect regions to the healthy regions in the attenuation correction by X-ray CT (especially on inspiration) of a phantom were better than those by TCT correction with an external gamma-ray source. Since X-ray CT is a widely used routine examination, our method could be used in many institutions. Therefore we did not evaluate the affect of the difference in the X-ray tube voltage, and the difference in the attenuation coefficient is reported to be small,[7,9–10] even when the tube voltage X-ray was changed.

As shown in the figures, attenuation corrected SPECT images were affected by the registration errors in X-ray CT and SPECT images. There have been a number of studies regarding adjustment of registration.[8,11–14] Image registration of brain SPECT imaging is easy, since it has a constant shape that is not affected by breathing, but in the myocardial study, our human results indicated that respiratory conditions influenced the SPECT images. Although registration errors are unavoidable when X-ray CT and SPECT are acquired separately, we felt that the registration errors would be minimal when three-dimensional registration software was used. It is necessary to investigate whether the attenuation corrected images with the registration errors would decrease accuracy or not. In other words, it is essential to verify that X-ray CT corrected myocardial SPECT imaging would increase accuracy in clinical use in future studies.

In conclusion, attenuation correction of myocardial SPECT with an X-ray CT image is a simple and potentially beneficial method in clinical use. Further clinical studies on a large number are necessary to verify the clinical benefit in the diagnosis of myocardial perfusion SPECT.

ACKNOWLEDGMENTS

The authors thank Dr. Ichiro Sogabe, Dr. Kana Sakamoto (Department of Radiology, Ehime Prefectural Imabari Hospital) and Mr. Akiyoshi Kinda (Toshiba Medical Engineering Laboratory) for their technical assistance.

REFERENCES

1. Murase K, Tanada S, Inoue T, Sugawara Y, Hamamoto K. Improvement of brain single photon emission tomography (SPET) using transmission data acquisition in a four-head SPET scanner. *Eur J Nucl Med* 1993; 20: 32–38.

2. Almeida P, Bendriem B, Dreuille O, Peltier A, Perrot C, Brulon V. Dosimetry of transmission measurements in nuclear medicine: a study using anthromorphic phantoms and thermoluminescent dosimeters. *Eur J Nucl Med* 1998; 25: 1435–1441.
3. Bocher M, Balan A, Krausz Y, Shrem Y, Lonn A, Wilk M, et al. Gamma camera-mounted anatomical X-ray tomography: technology, system characteristics and first images. *Eur J Nucl Med* 2000; 27: 619–627.
4. Patton JA, Delbeke D, Sandler MP. Image fusion using an integrated, dual-head coincidence camera with X-ray tube-based attenuation maps. *J Nucl Med* 2000; 41: 1364–1368.
5. Kalki K, Blankespoor SC, Brown JK, Hasegawa BH, Dae MW, Shin M, et al. Myocardial perfusion imaging with a combined x-ray CT and SPECT system. *J Nucl Med* 1997; 38: 1535–1540.
6. Takahashi Y, Murase K, Higashino H, Sogabe I, Sakamoto K. Receiver operating characteristic (ROC) analysis of image reconstructed with iterative expectation maximization algorithms. *Ann Nucl Med* 2001; 15: 521–525.
7. Motomura N, Ichihara T, Satou T, Kinda A, Kitano T, Kubo H. Examination of the SPECT attenuation correction using the X-ray CT image [abstract]. *KAKU IGAKU (Jpn J Nucl Med)* 1999; 36: 617.
8. Ardekani BA, Braun M, Hutton BF, Kanno I, Iida H. A Fully Automatic Multimodality Image Registration Algorithm. *J Comput Assist Tomogr* 1995; 19: 615–623.
9. Fleming JS. A technique for using CT images in attenuation correction and quantification in SPECT. *Nucl Med Commun* 1989; 10: 83–97.
10. Kamel E, Hany TF, Burger C, Treyer V, Lonn AHR, von Schulthess GK. CT vs ^{68}Ge attenuation correction in a combined PET/CT system: evaluation of the effect of lowering the CT tube current. *Eur J Nucl Med* 2002; 29: 346–350.
11. Murase K, Tanada S, Inoue T, Sugawara Y, Hamamoto K. Effect of misalignment between transmission and emission scans on SPECT images. *J Nucl Med Technol* 1993; 21: 152–156.
12. Stone CD, McCormick JW, Gilland DR, Greer KL, Coleman RE, Jaszczak RJ. Effect of registration errors between transmission and emission scans on a SPECT system using sequential scanning. *J Nucl Med* 1998; 39: 365–373.
13. Koole M, D'Asseler Y, Van LK, Van de Walle R, Van de Wiele C, Lemahieu I. MRI-SPET and SPET-SPET brain co-registration: Evaluation of the performance of eight different algorithms. *Nucl Med Commun* 1999; 20: 659–669.
14. Suga K, Matsunaga N, Kawakami Y, Furukawa M. Phantom study of fusion image of CT and SPECT with body-contour generated from Compton scatter sources. *Ann Nucl Med* 2000; 14: 271–277.